Since January 2020 Elsevier has created a COVID-19 resource centre with free information in English and Mandarin on the novel coronavirus COVID-19. The COVID-19 resource centre is hosted on Elsevier Connect, the company's public news and information website.

Chaos, Solitons and Fractals 139 (2020) 110042

Contents lists available at ScienceDirect

Chaos, Solitons and Fractals

Nonlinear Science, and Nonequilibrium and Complex Phenomena

journal homepage: www.elsevier.com/locate/chaos

A mathematical study on the spread of COVID-19 considering social distancing and rapid assessment: The case of Jakarta, Indonesia

Dipo Aldila[a,*], Sarbaz H.A. Khoshnaw[b], Egi Safitri[a], Yusril Rais Anwar[a], Aanisah R.Q. Bakry[a], Brenda M. Samiadji[a], Demas A. Anugerah[a], M. Farhan Alfarizi GH[a], Indri D. Ayulani[a], Sheryl N. Salim[a]

[a] Department of Mathematics, Universitas Indonesia, Depok 16424, Indonesia
[b] Department of Mathematics, University of Raparin, Ranya 46012, Kurdistan Region of Iraq

ARTICLE INFO

Article history:
Received 22 May 2020
Accepted 18 June 2020
Available online 28 June 2020

MSC:
34D05
92D30

Keywords:
COVID-19
Asymptomatic cases
Social distancing
Rapid test
Basic reproduction number
Backward bifurcation

ABSTRACT

The aim of this study is to investigate the effects of rapid testing and social distancing in controlling the spread of COVID-19, particularly in the city of Jakarta, Indonesia. We formulate a modified susceptible exposed infectious recovered compartmental model considering asymptomatic individuals. Rapid testing is intended to trace the existence of asymptomatic infected individuals among the population. This asymptomatic class is categorized into two subclasses: detected and undetected asymptomatic individuals. Furthermore, the model considers the limitations of medical resources to treat an infected individual in a hospital. The model shows two types of equilibrium point: COVID-19 free and COVID-19 endemic. The COVID-19-free equilibrium point is locally and asymptotically stable if the basic reproduction number ($\mathscr{R}_0$) is less than unity. In contrast, COVID-19-endemic equilibrium always exists when $\mathscr{R}_0 > 1$. The model can also show a backward bifurcation at $\mathscr{R}_0 = 1$ whenever the treatment saturation parameter, which describes the hospital capacity, is larger than a specific threshold. To justify the model parameters, we use the incidence data from the city of Jakarta, Indonesia. The data pertain to infected individuals who self-isolate in their homes and visit the hospital for further treatment. Our numerical experiments indicate that strict social distancing has the potential to succeed in reducing and delaying the time of an outbreak. However, if the strict social distancing policy is relaxed, a massive rapid-test intervention should be conducted to avoid a large-scale outbreak in the future.

1. Introduction

Coronavirus disease 2019, or COVID-19, is an infectious disease caused by a new type of coronavirus named severe acute respiratory syndrome coronavirus 2 (SARS-CoV-2), which is known to have originated in the city of Wuhan, China in December 2019 [1]. This virus is transmitted from human to human and has spread widely across China and 214 other countries and territories. It is spread through droplets that exit the nose or mouth when a person infected with COVID-19 coughs or exhales. These droplets then land and settle on surrounding objects and surfaces. If a person who touches any of those objects or surfaces then touches their eyes, nose, or mouth, they may become infected. Transmission can also occur if a person inhales droplets from a cough or breath of a person infected with COVID-19 [2]. On March 12, 2020, the World Health Organization (WHO) declared COVID-19 as a pandemic. Till May 16, 2020, there were 4,338,658 cases and 297,119 deaths worldwide. In Indonesia, there were 17,025 positive COVID-19 cases and 1,089 deaths till May 13, 2020 [2].

According to the WHO [3], COVID-19 generally has an incubation period of 5–6 days, with a range of 1–14 days. The symptoms of COVID-19 are nonspecific and vary widely, ranging from no symptoms to severe pneumonia and eventual death. Based on specific cases, some of the symptoms of COVID-19 include fever, dry cough, fatigue, nasal congestion, diarrhea, and headache. People who are at high risk for severe illness include those aged 60 years and over and those with hypertension, diabetes, cardiovascular problems, cancer, or a chronic respiratory disease. The mortality rate increases with age, with the highest death rate among people aged over 80 years. In children, the disease is relatively rare.

Each country is at a different stage of the epidemic. In most countries where the spread of the virus has caused outbreaks with exponential growth, governments have called for physical distancing and movement restrictions, commonly known as *lockdown*, to

* Corresponding author.
E-mail address: aldiladipo@sci.ui.ac.id (D. Aldila).

https://doi.org/10.1016/j.chaos.2020.110042
0960-0779/

slow the spread of the COVID-19 outbreak [4]. Some of these countries include China, Italy, and the United Kingdom. Moreover, there are some countries that have managed to handle the COVID-19 outbreak without a lockdown; one such country is South Korea. Based on a report in [5], South Korea conducted massive numbers of polymerase chain reaction tests, which reached 726,747 by May 15, 2020 [6].

In addition to death, this pandemic has also had negative psychological, economic, and social impacts globally. The COVID-19 pandemic has resulted in changes in the work environment, indirectly affecting gender inequality, and an increased risk of suicide owing to lockdown, social distancing, and economic crisis [7]. Panic in communities may be reduced by educating the public regarding the predictions of the COVID-19 epidemic and the interventions that must be conducted. Communities must also unite and work together to help governments overcome the epidemic by following the guidelines provided by the relevant authorities [7].

Several mathematical models have been proposed by several authors to understand the spreading mechanism of COVID-19. In [8–14], the authors proposed a modified susceptible-exposed-infected-recovered (SEIR) model to understand the effects of undetected infection, hospitalization, and quarantine. The model was analyzed to determine the equilibria and the basic reproduction number. Parameter estimation was conducted by the authors in [11,12,15,16] using a statistical approach involving a Bayesian or Markov Chain Monte Carlo method. In addition to compartmental deterministic modeling, the spread of COVID-19 can be predicted statistically using a time-series approach [17–19]. A time-series model is effective owing to its ability to accommodate the factors influencing the spread of COVID-19 that cannot be calculated using other statistical approaches [17]. A frequently used time-series model is the autoregressive integrated moving average (p, d, q).

In this study, we propose a modified SEIR model that considers asymptomatic cases. These asymptomatic cases describe a hidden case in the field. As an intervention, rapid testing has been implemented by many countries to detect infected individuals in this asymptomatic group. Therefore, we categorize our asymptomatic individuals into two groups: detected and undetected. Furthermore, we also accommodate the limitation of resources for medical treatment. This is an extremely important factor that will have an essential role in a successful eradication of COVID-19. Many countries are not ready for an exponential growth of COVID-19 cases because many hospitals will become overwhelmed by the high number of patients. To validate the model, COVID-19 incidence data from the city of Jakarta are used for parameter estimation. The basic reproduction number is calculated, and a sensitivity analysis of the model is conducted. The model is then used to predict the effects of social and physical distancing to stop the spreading of COVID-19, and to monitor the effects of the plan to gradually ease social distancing guidelines of the government in Jakarta.

The remainder of this paper is organized as follows. In Section 2, the construction of the SEA_uA_dIR compartmental model is described. Next, the mathematical properties of the model, such as the equilibrium points, basic reproduction number, and existence of backward bifurcation, are detailed in Section 3. In Section 4, we explain the real-world problem using the incidence data of Jakarta, Indonesia. A discussion on the basic reproduction number and the results of the sensitivity analysis are provided in Section 6. Finally, some conclusions are presented in Section 7.

2. Proposed SEA_uA_dIR model

The objective of our study is to analyze the effect of rapid testing and self-monitored isolation, and to predict the long-term dynamics of the incidence data of Jakarta, Indonesia. To achieve these purposes, our model should consider asymptomatic cases, as well as a parameter describing a rapid test intervention. To achieve this, let us divide the human population into six categories based on their health status:

(i) Susceptible population ($S(t)$) := Group of susceptible individuals.
(ii) Exposed population ($E(t)$) := Group of individuals, who are already infected by COVID-19, but not yet infective.
(iii) Infected population ($I(t)$) := Group of an infected individuals who shows symptoms and are treated in a hospital. Limited social interactions occur in this group of individuals.
(iv) Asymptomatic undetected population ($A_u(t)$) := Infected population having a capability to transmit COVID-19, do not show any symptoms, and undetected by the government. Such individuals have a larger probability of spreading the disease compared with I and A_d.
(v) Asymptomatic detected population ($A_d(t)$) = Individuals in this category are similar to those in A_u in terms of their health status, but have already been detected by the government through a swab-test, rapid test, or other tests. Although this group of individuals has the capability of spreading the disease, they do not isolate themselves in a hospital owing to a limited hospital capacity. Therefore, a monitored self-isolation is applicable to them.
(vi) Recovered population ($R(t)$) := Recovered individuals with a short-term immunity to COVID-19.

Therefore:

$$N = S + E + I + A_u + A_d + R.$$

We make the following assumptions for the formulation of the model.

a) The human population is homogeneously mixed.
b) Rapid testing for COVID-19 is implemented to identify infected individuals among the population and is provided to an individual who does not show any symptoms. Therefore, this rapid testing is given to an individuals in all types of compartments, except I.
c) Asymptomatic undetected individuals can socialize more than those in I and A_d owing to the absence of symptoms .
d) Disease induced death only exists for individuals in I.
e) Infected individuals in hospitals have a chance to recover faster than infected individuals who have not received medical treatment. Caused by a limited number of beds or other medical resources in a hospital, we assume that the additional recovery rate for an infected individual in the hospital is saturated with respect to the number of patients that need to be handled, using the saturated parameter b.

Using the transmission diagram given in Fig. 1 and the aforementioned assumptions, the model to describes the transmission of COVID-19 by considering rapid testing and asymptomatic cases is expressed as the following systems of equation.

$$\begin{aligned}
S' &= \Lambda - \beta S(A_u + \xi_i I + \xi_a A_d) - \mu S + \delta R,\\
E' &= \beta S(A_u + \xi_i I + \xi_a A_d) - \alpha E - \mu E,\\
A_u' &= p\alpha E - \nu A_u - \gamma_0 A_u - \mu A_u,\\
A_d' &= \nu A_u - \gamma_0 A_d - \eta A_d - \mu A_d,\\
I' &= (1-p)\alpha E + \eta A_d - \left(\gamma_0 + \frac{\gamma_1}{1+bI}\right) I - \mu I - \phi I,\\
R' &= \gamma_0(A_u + A_d) + \left(\gamma_0 + \frac{\gamma_1}{1+bI}\right) I - \mu R - \delta R.
\end{aligned} \tag{1}$$

Here, Λ, β, μ, and ϕ are the natural recruitment rate, infection rate, natural death rate, and death rate from COVID-19, respec-

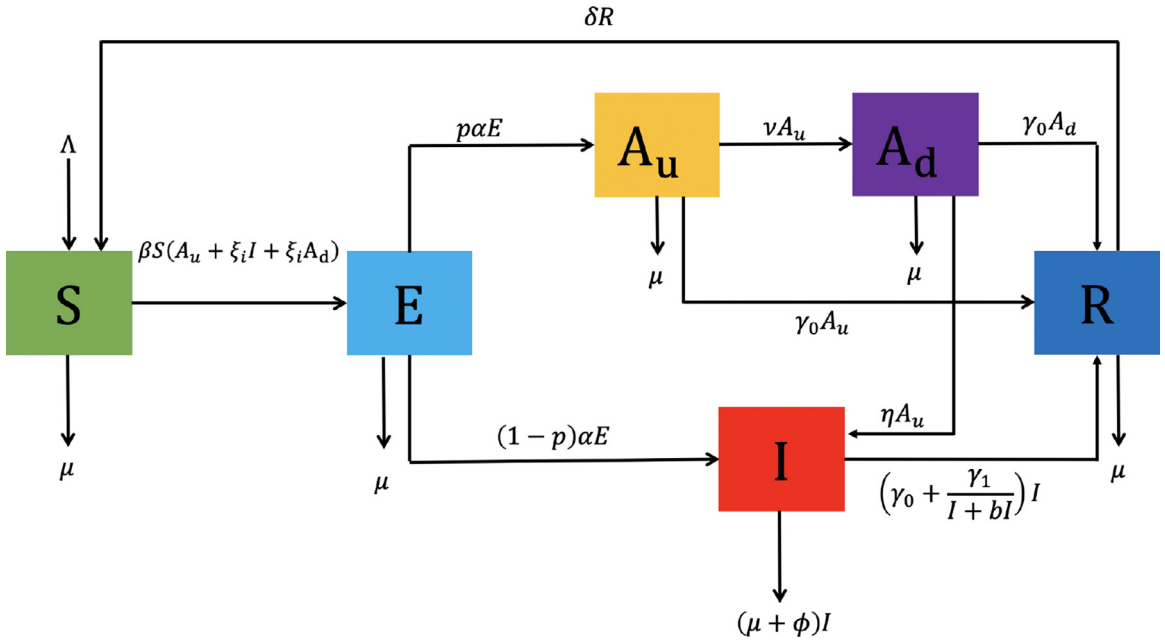

Fig. 1. Transmission diagram of COVID-19 spread considering asymptomatic undetected cases and rapid-test.

tively. ξ_i and ξ_a represent the reduction of β for I and A_d, respectively, owing to isolation at home or in a hospital. Furthermore, α, γ_0, and δ denote the progression rate of COVID-19 based on its incubation period, natural recovery rate, and disappearance of temporal immunity, respectively. Note that p describes the proportion of exposed individuals who have progressed into asymptomatic individuals, γ_1 is the enhancement of natural recovery rate owing to treatment in a hospital, η is the rate of hospitalization from A_d to I, and ν is the effort required for early detection of COVID-19 infection. Note that system (1) is supplemented with an non-negative initial condition:

$$S(0) \geq 0,\ E(0) \geq 0,\ I(0) \geq 0,\ A_u(0) \geq 0,\ A_d(0) \geq 0,\ R(0) \geq 0.$$

$$\mathcal{R}_0 = \frac{\beta\Lambda\alpha[\xi_i(\eta\nu + (1-p)(\mu+\gamma_0)(\mu+\eta+\nu+\gamma_0) + p(\nu\xi_a + \eta + \mu + \gamma_0)(\mu+\phi+\gamma_0+\gamma_1))]}{\mu(\mu+\phi+\gamma_0+\gamma_1)(\mu+\nu+\gamma_0)(\mu+\eta+\gamma_0)(\alpha+\mu)}. \tag{4}$$

3. Model analysis

3.1. Basic properties of the model

It is not difficult to prove that all variables in system (1) remain nonnegative for all time $t \geq 0$ as long as the initial conditions are nonnegative. Next, we show that our model is well-posed in biological meaning. Let us consider the possible region

$$\mathscr{D} = \left\{(S, E, I, A_u, A_d, R) \in \mathbb{R}^6_+ : N \leq \frac{\Lambda}{\mu}\right\}.$$

Summation of all rates of change for each variable in system (1) yields

$$\frac{dN}{dt} = \Lambda - \mu N - \psi I \leq \Lambda - \mu N. \tag{2}$$

Clearly, if $N > \frac{\Lambda}{\mu}$, then we have that $\frac{dN}{dt} < 0$. Since $\frac{dN}{dt}$ is bounded by $\Lambda - \mu N$, we have that $N(t) \leq N(0)e^{-\mu t} + \frac{\Lambda}{\mu}\left(1 - e^{-\mu t}\right)$. Furthermore, we have that $N(0) \leq \frac{\Lambda}{\mu} \rightarrow N(t) \leq \frac{\Lambda}{\mu}$. Additionally, it can be seen that every solution of our COVID-19 model in (1) with the initial condition in $\mathscr{D}$ will remain in $\mathscr{D}$ for all $t > 0$. Therefore, we have that $\mathscr{D}$ is positively invariant and attracting. Hence, the COVID-19 model in (1) is well-posed.

3.2. Qualitative analysis of the model

3.2.1. COVID-19 free equilibrium and the basic reproduction number

Considering the right-hand side of system (1) is equal to zero, we have two types of equilibrium points for system (1). The first equilibrium is the COVID-19 free equilibrium point, which is given by

$$\mathscr{E}_0 = (S, E, I, A_u, A_d, R) = \left(\frac{\Lambda}{\mu}, 0, 0, 0, 0, 0\right). \tag{3}$$

Using the next-generation matrix approach [20], the basic reproduction number of system (1) is given by (*See* Appendix A *for the derivation of the* $\mathscr{R}_0$)

From the results in [21], we have the local stability criteria of $\mathscr{E}_0$ depending on $\mathscr{R}_0$ in the following theorem.

Theorem 1. *The COVID-19 free equilibrium* $\mathcal{E}_0$ *is locally asymptotically stable if* $\mathcal{R}_0 < 1$, *and unstable otherwise.*

Threshold quantity $\mathscr{R}_0$ presents the expected number of new COVID-19 infections generated from one primary infection into an absolute susceptible population during a single infection period. From the results of Theorem 1, it can be shown that COVID-19 can be eliminated from the population if $\mathscr{R}_0 < 1$. Please note that $\mathscr{R}_0$ in (4) is a basic reproduction number when a rapid test is implemented. When a rapid test is not implemented into the model, then $\mathscr{R}_0$ in (4) is reduced to the following:

$$\mathscr{R}_0^* = \frac{\Lambda}{\mu} \times \frac{\beta}{\alpha+\mu} \times \alpha\left[\frac{(1-p)\xi_i}{\mu+\phi+\gamma_0+\gamma_1} + \frac{p}{\mu+\gamma_0}\right]. \tag{5}$$

This shows the multiplication among the total human population when no COVID-19 exists, ratio between the infection rate and exposed/incubation period of category E, and infection period of categories A_u and I. It is easy to see that reducing $\mathscr{R}_0^*$ is highly related to reducing β, which can be implemented by reducing the contact probability through lockdown or social distancing, and reducing ξ_i by conducting a proper quarantine procedure in a hospital, such

that $\xi_i \to 0$. Another way to reduce $\mathscr{R}_0^*$ is by increasing the recovery rate owing to hospitalization (γ_1). Further discussion on the complete $\mathscr{R}_0$ is provided in Section 5.

3.3. The COVID-19 endemic equilibrium points

The endemic equilibrium point of system (1) is expressed as

$$\mathcal{E}_1 = \left(S^*, E^*, I^*, A_u^*, A_d^*, R^*\right), \tag{6}$$

where $S^*, E^*, A_u^*, A_d^*, R^*$ expressed as a functions of I^* are described in Appendix B, whereas I^* is taken from the positive roots of the following third order polynomial :

$$\mathcal{P}(I) = a_3 I^3 + a_2 I^2 + a_1 I + a_0 = 0, \tag{7}$$

with

$$a_3 = \frac{b^2\beta(1-p)\xi_i(\mu+\gamma_0)(\mu+\eta+\nu+\gamma_0) + (\mu+\phi+\gamma_0)(\nu\xi_a+\eta+\mu+\gamma_0)}{(1-p)\alpha\delta\phi\gamma_0(\mu+\eta+\nu+\gamma_0) + \mu(\mu+\phi+\gamma_0)(\mu+\nu+\gamma_0)(\mu+\eta+\gamma_0)(\alpha+\delta+\mu)},$$
$$a_0 = (\delta+\mu)\mu(\mu+\phi+\gamma_0+\gamma_1)(\mu+\nu+\gamma_0)(\mu+\eta+\gamma_0)(\alpha+\mu)(1-\mathcal{R}_0).$$

Here, a_2 and a_1 have significantly long expressions and are therefore omitted in this study. Because a_3 is always positive, and $a_0 < 0$ if $\mathscr{R}_0 > 1$, we have the following theorem.

Theorem 2. *System (1) has always a COVID-19 endemic equilibrium pint whenever $\mathscr{R}_0 > 1$.*

Proof. Note that $\mathcal{P}(I)$ has one zero roots whenever $a_0 = 0 \iff \mathscr{R}_0 = 1$, whereas the other two roots can be positive, negative, or even imaginary. Let us consider the most extreme case in which we have no positive roots. Because we have $a_3 > 0$, we then have $\lim_{I\to-\infty}\mathcal{P}(I) = -\infty$ and $\lim_{I\to\infty}\mathcal{P}(I) = \infty$. Therefore, when $a_0 < 0 \iff \mathscr{R}_0 > 1$, we have the polynomial is being translated downward and providing one positive root. This completes the proof. □

Theorem 1 and 2 indicate that $\mathscr{R}_0$ become the endemic threshold; this occurs because,when $\mathscr{R}_0 < 1$, we have that the COVID-19 free equilibrium is stable; however, when $\mathscr{R}_0 > 1$, then we have at least one positive COVID-19 endemic equilibrium. Furthermore, since the polynomial is third-order , we have at most three COVID-19 endemic equilibrium. Next, we analyze the possibility of having a COVID-19 endemic equilibrium when $\mathscr{R}_0 < 1$. The results stated in the following theorem.

Theorem 3. *Whenever $b > b^*$, where*

$$b^* = \frac{\beta^*((1-p)\xi_i(\mu+\gamma_0)(\eta+\mu+\nu+\gamma_0) - \eta\nu\xi_i - p(\mu+\phi+\gamma_0+\gamma_1)(\nu\xi_a+\eta+\mu+\gamma_0))k_{b_1}}{(\mu+\delta)((1-p)(\mu+\gamma_0)(\eta+\mu+\nu+\gamma_0) - \eta\nu)k_{b_2}}, \tag{8}$$

and

$$\beta^* = \frac{\mu(\mu+\phi+\gamma_0+\gamma_1)(\mu+\nu+\gamma_0)(\mu+\eta+\gamma_0)(\alpha+\mu)}{\Lambda\alpha[\xi_i(\eta\nu+(1-p)(\mu+\gamma_0)(\mu+\eta+\nu+\gamma_0)) + p(\mu+\phi+\gamma_0+\gamma_1)(\nu\xi_a+\eta+\mu+\gamma_0)]},$$

system (1) has a COVID-19 endemic equilibrium point when $\mathscr{R}_0 < 1$.

Proof. For the proof of this theorem, please refer to Appendix C. □

As a direct consequence of Theorem 3 and 2, we have the following corollary.

Corollary 1. *System (1) has two endemic equilibrium points when $\mathscr{R}_0 < 1$ if $b > b^*$.*

We end this section with the following theorem to describe the condition of a backward bifurcation of system (1).

Theorem 4. *System (1) undergoes backward bifurcation in $\mathscr{R}_0 = 1$ if $b > b^*$. In contrast , it undergoes forward bifurcation in $\mathscr{R}_0 = 1$ if $b < b^*$.*

Proof. For the proof of Theorem, please see Appendix D □

4. Parameter estimation: case study of the city of Jakarta, Indonesia

4.1. COVID-19 incidence data of Jakarta

Jakarta is the capital of Indonesia, with a population of 10,374,235 as of 2019, and a population growth rate of 0.94% per year. Jakarta consists of six sub-governments, namely South, East, West, North and Central Jakarta, and the Thousand Islands. The largest population is in East Jakarta at 2,916,020 people.

The first COVID-19 case in Jakarta was recorded on March 3, 2020, from a patient who had contact with Japanese citizens (whom later on was confirmed to be positive for COVID-19). Social distancing is the most preferred action by the Jakarta city government to reduce the spread of COVID-19. This rule has been applied since April 10, 2020, which is based on Jakarta Governor Regulation No 33/2020. The regulation requires the closure of schools, public facilities such as malls, and many other places that might potentially have a gathering of people in the same location .

The data used in this study are COVID-19 incident data from Jakarta, collected from March 3, to May 10, 2020. These data can be divided into two types of active cases, namely active cases that must be treated in a hospital (I) and independent isolation at home (A_d). The incident data used are listed in Table 1.

4.2. Estimation of epidemiological parameters

To conduct the parameter estimation for data-driven from Jakarta, Indonesia, owing to the short-term of the data, we consider model (1) but neglect the natural newborns, natural death rate, and the drop out rate from recovered compartment due to the possibility that a temporal immunities will expire . Based on this assumption, Model (1) now reads as follows:

$$\begin{aligned}
S' &= -\beta S(A_u + \xi_i I + \xi_a A_d),\\
E' &= \beta S(A_u + \xi_i I + \xi_a A_d) - \alpha E,\\
A_u' &= p\alpha E - \nu A_u - \gamma_0 A_u,\\
A_d' &= \nu A_u - \eta A_d - \gamma_0 A_d,\\
I' &= (1-p)\alpha E + \eta A_d - \left(\gamma_0 + \frac{\gamma_1}{1+bI}\right)I - \phi I,\\
R' &= \gamma_0(A_u + A_d) + \left(\gamma_0 + \frac{\gamma_1}{1+bI}\right)I.
\end{aligned} \tag{9}$$

To conduct a parameter estimation, we divided our data based on the date that strict social distancing in Jakarta was first time implemented. The first interval is from March 3, until April 10, 2020.

Table 1
COVID-19 incidence data from Jakarta, collected from 03 March 2020 until 10 May 2020.

Data	I	A_d	Data	I	A_d	Data	I	A_d
3 March '20	2	0	26 March '20	324	113	18 April '20	1769	670
4 March '20	2	0	27 March '20	346	132	19 April '20	1839	695
5 March '20	4	0	28 March '20	364	134	20 April '20	1826	752
6 March '20	4	0	29 March '20	435	151	21 April '20	1935	753
7 March '20	4	0	30 March '20	449	151	22 April '20	1985	815
8 March '20	4	0	31 March '20	451	157	23 April '20	2010	888
9 March '20	31	0	1 April '20	499	176	24 April '20	1988	959
10 March '20	31	0	2 April '20	565	195	25 April '20	1947	1050
11 March '20	33	0	3 April '20	627	209	26 April '20	1952	1099
12 March '20	57	0	4 April '20	691	223	27 April '20	1950	1169
13 March '20	65	0	5 April '20	685	279	28 April '20	2024	1206
14 March '20	70	0	6 April '20	783	317	29 April '20	2002	1238
15 March '20	84	0	7 April '20	895	338	30 April '20	2073	1272
16 March '20	78	7	8 April '20	976	357	1 May '20	2151	1312
17 March '20	83	27	9 April '20	1077	405	2 May '20	2089	1304
18 March '20	91	42	10 April '20	1139	433	3 May '20	2062	1323
19 March '20	121	57	11 April '20	1152	441	4 May '20	2080	1330
20 March '20	125	66	12 April '20	1277	468	5 May '20	2146	1370
21 March '20	157	71	13 April '20	1370	521	6 May '20	2195	1381
22 March '20	177	77	14 April '20	1385	558	7 May '20	2196	1431
23 March '20	225	79	15 April '20	1424	613	8 May '20	2281	1426
24 March '20	260	109	16 April '20	1601	619	9 May '20	2312	1442
25 March '20	290	112	17 April '20	1727	643	10 May '20	2360	1533

During this interval, we found that the best fit parameters are :

$$\beta = 1.44 \times 10^{-7},\ \eta = 0.19,\ \nu = 0.367,\ \xi_i = 0.2,\ \xi_a = 0.5,\ \alpha = 0.25,$$
$$\gamma_0 = 0.27,\ \gamma_1 = 0.23,\ \phi = 0.06,\ p = 0.42,\ b = 10^{-4}.$$

With these parameters, we have that $\mathscr{R}_0$ in Jakarta during this interval is **1.75**. This indicates that COVID-19 has a big potency to be endemic in Jakarta if accurate, precise, and fast policies were not carried out soon. During the second interval, after the strict social distancing implemented, we set other parameters constant, whereas β and η should be re-estimated. In this second interval from April 11 until May 10, we have $\beta = 0.94 \times 10^{-7}$ and $\eta = 0.06$. This data gives $\mathscr{R}_0 = \mathbf{1.22}$ in the second interval. It can be seen that β was reduced by 34%, which indicates the effect of the social distancing policy. On the other hand, η reduced by 68.4%, since the number of infected individual continued increasing in the hospitals. Therefore, the transition from A_d to I need to be reduced because of the limitation on the hospital capacity. The results of the parameter estimation for system (1) with respect to the incidence data in Jakarta are given in Fig. 2.

5. Discussion of $\mathscr{R}_0$ and sensitivity analysis

We conduct numerical experiments in this section in three scenarios. The aim of the first experiment is to analyze the elasticity of $\mathscr{R}_0$. From Theorem 1, 2, 3 and 4, it is clear to see that our model is dependent on the size of $\mathscr{R}_0$. Understanding how $\mathscr{R}_0$ behave when the parameters change will help acchieve a more effective intervention to control the spread of COVID-19. The second experiment aims to see how the estimated parameter from the incidence data in Jakarta might exhibit a backward bifurcation when the quality and size of the patients handled in the hospital getting worse. The final experiment is the sensitivity analysis to determine the most significant parameters in determining the dynamics of each variable.

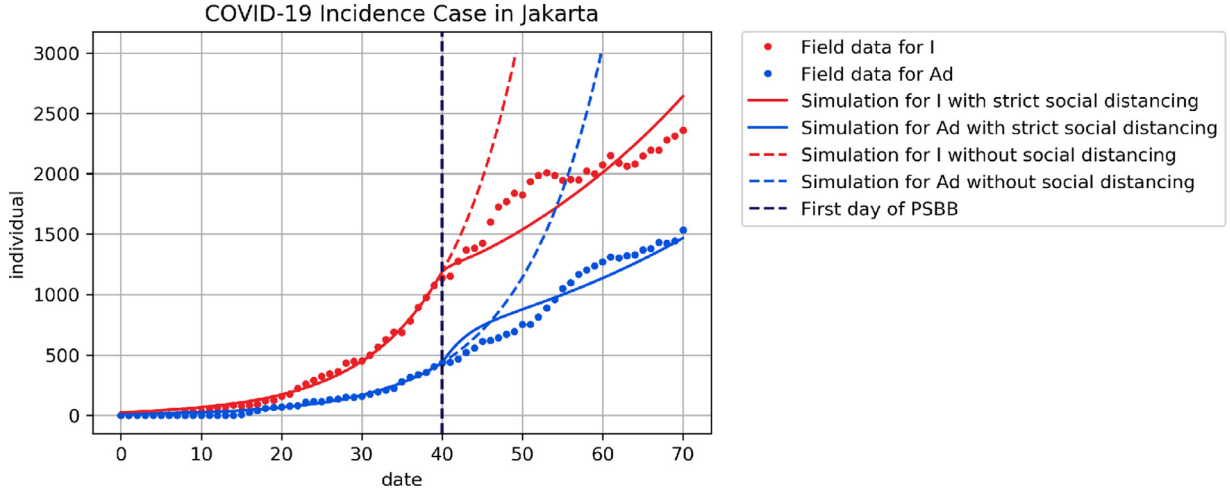

Fig. 2. Comparison between COVID-19 incidence data of Jakarta from March 3, - May 10, 2020 in Jakarta (dotted) with the simulation of A_d and I from the model in system (9).

Table 2
Elasticity value of $\mathscr{R}_0$ with respect to the parameters in system (1).

ω	$\Gamma_\omega^{\mathscr{R}_0}$	ω	$\Gamma_\omega^{\mathscr{R}_0}$
Λ	1	β	1
μ	-1.000262026	δ	0
η	−0.07563488004	ν	−0.2174486541
ξ_1	0.2088834091	ξ_a	0.2268945826
α	0.0001685711554	γ_0	−0.5986593834
γ_1	−0.08578494311	ϕ	−0.02237868082
p	0.6929432923	b	0

5.1. Elasticity of $\mathscr{R}_0$

To perform the elasticity analysis on $\mathscr{R}_0$, we calculate the normalized forward sensitivity index of $\mathscr{R}_0$ using the following formula :

$$\Gamma_\omega^{\mathscr{R}_0} = \frac{\partial \mathscr{R}_0}{\partial \omega} \times \frac{\omega}{\mathscr{R}_0}, \tag{10}$$

where ω is the set of parameters in system (1). For example, the elasticity index of $\mathscr{R}_0$ with respect to α is given by

$$\Gamma_\alpha^{\mathscr{R}_0} = \frac{\partial \mathscr{R}_0}{\partial \alpha} \times \frac{\alpha}{\mathscr{R}_0} = \frac{\mu}{\alpha + \mu}.$$

In a similar way, we can find all elasticity indices of $\mathscr{R}_0$ for the remaining of parameters. Substituting the parameters value found from Section 4 and assuming $\Lambda = 10,467,629/(65 \times 365)$, $\mu = 1/(65 \times 365)$ and $\delta = 1/90$, the elasticity value of all parameters in system (1) respect to $\mathscr{R}_0$ is given in Table 2.

The positive and negative signs in Table 2 indicate increasing and decreasing values of $\mathscr{R}_0$ with respect to the parameters, respectively. Therefore, we can state that $\mathscr{R}_0$ increases when Λ, β, ξ_i, ξ_a, α or p increases. In the other hand, whenever μ, η, ν, γ_0, γ_1, or ϕ increases, then $\mathscr{R}_0$ will decreases. Furthermore, for an example, since $\Gamma_\nu^{\mathscr{R}_0} = -0.2174486541$, increasing ν for 10% will reduce $\mathscr{R}_0$ 2.174486541%. A similar interpretation is given for the remaining parameters in Table 2. It is interesting to see that the saturation parameter b, which describes the capacity of the hospital or the number of a medical officers, does not affect the size of $\mathscr{R}_0$ since $\Gamma_b^{\mathscr{R}_0} = 0$. However, b plays an important role in determining whether the system (1) undergoes a forward or backward bifurcation when $\mathscr{R}_0 = 1$. From Table 2, it can be seen that β is the most positive significant parameter that can be used to control $\mathscr{R}_0$. Therefore, social/physical distancing is a very reasonable intervention to control the spread of COVID-19. Furthermore, it can be seen that reducing ξ_i and ξ_a will reduce $\mathscr{R}_0$, which indicates that a better the reduction of contact from infected humans through isolation in the hospital or at home is able to reduce $\mathscr{R}_0$. The most negative index of $\mathcal{R}_0$ is given by μ. However, this parameter can not be changed in the field. The most negative index parameter that is controllable in the field is ν, which describes the rate of the rapid testing. Therefore, we can conclude that more massive the government endeavor is to find the asymptomatic individuals, and the more such individuals are asked to isolate independently at home, the more we can reduce $\mathscr{R}_0$. Furthermore, we can see that increasing the additional recovery rate caused by hospitalization (γ_1) will reduce $\mathscr{R}_0$.

Fig. 3 presents an area for a combination between ν and β that will determine the size of $\mathscr{R}_0$. It can be seen that the increased value of β will increase $\mathscr{R}_0$, while an increased value of ν will reduce $\mathscr{R}_0$. The area of β can differ into three intervals. The first interval is when $\beta \in (1.010006455 \times 10^{-7}, \infty)$. In this interval, $\mathscr{R}_0$ is always larger than unity for all value of ν between 0 and 1. This means that the intervention of rapid tests will not make the COVID-19 free equilibrium stable. The second interval is

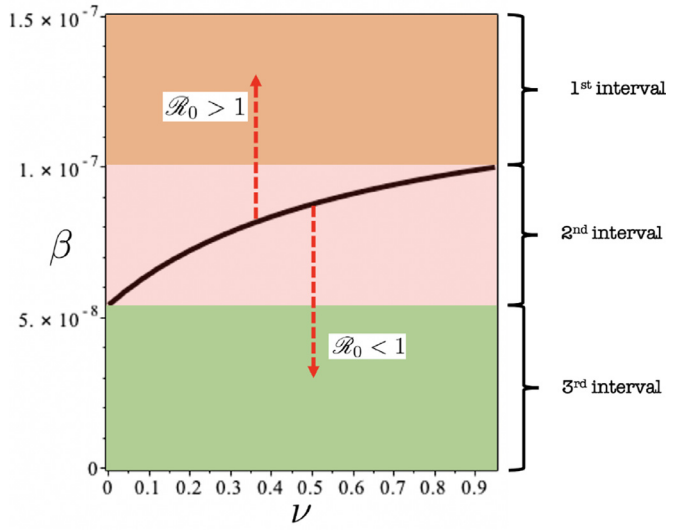

Fig. 3. Sensitivity area of $\mathscr{R}_0$ with respect to ν and β. The black curve indicates $\mathscr{R}_0 = 1$.

when $\beta \in (5.421388711 \times 10^{-8}, 1.010006455 \times 10^{-7})$. In this area, a combination of ν and β should be considered carefully to reach the condition of a stable COVID-19 free equilibrium point. For more precisely, for a random $\beta = \beta_0$ in the second interval, it needs $\nu > \nu^*$ where

$$\nu* = -\frac{(\eta + \mu + \gamma_0)[\Lambda\alpha\phi\beta_0\xi_i(1-p)(\mu+\gamma_0) + c_1]}{\Lambda\alpha\phi\beta_0(\mu\xi_a - \mu\xi_i + \phi\xi_a + \gamma_0\xi_a - \gamma_0\xi_i + \gamma_1\xi_a)p + c_2},$$

with

$$c_1 = (\mu + \phi + \gamma_0 + \gamma_1)\left(\Lambda\alpha\phi\beta_0 p - \alpha\mu^2 - \alpha\mu\gamma_0 - \mu^3 - \mu^2\gamma_0\right),$$
$$c_2 = (\mu + \eta + \gamma_0)(\Lambda\alpha\phi\beta_0\xi_i - \mu(\mu + \phi + \gamma_0 + \gamma_1)(\mu + \alpha)),$$

such that COVID-19 eradicated from the community. For an example, if $\beta_0 = 0.9 \times 10^{-7}$, then it requires $\nu > 0.5630546276$ to achieve a stable COVID-19 free equilibrium point. The last interval is when $\beta \in [0, 5.421388711 \times 10^{-8})$. In the third interval, the intervention of rapid testing is not needed to reach a stable COVID-19 free equilibrium point. However, giving a positive value of ν will accelerate the time needed to achieve a stable COVID-19 free equilibrium point.

5.2. Forward and backward bifurcation

From Theorem 4, system (1) undergoes backward bifurcation in $\mathscr{R}_0 = 1$ if $b < b^*$. In the other hand, when $b > b^*$, then system (1) undergoes forward bifurcation in $\mathscr{R}_0 = 1$. Using estimated parameters value from previous section, we have that $\mathscr{R}_0 = 1$ when $\beta = 8.599684570 \times 10^{-8}$, and $b^* = 1/573$. Therefore, we have that our system (1) undergoes forward bifurcation when $\mathscr{R}_0 = 1$ since $b = 1/10000$, which illustrated in Fig. 4(a). On the other hand, backward bifurcation appears when we choose $b = 1/100$, which describes a low capacity of the hospital to take care of the infected individual. This is illustrated in Fig. 4(b).

5.3. Sensitivity analysis

We compute the local sensitivity for our suggested model equations of COVID-19 in system (1). The computational results here are obtained using three different techniques: non-normalizations, half normalizations and full normalizations using *SimBiology* Toolbox for MATLAB; see Figs. 5–7. Interestingly, the results provide us further understanding to the model and give ones to identify the critical model parameters. Based on non-normalization technique,

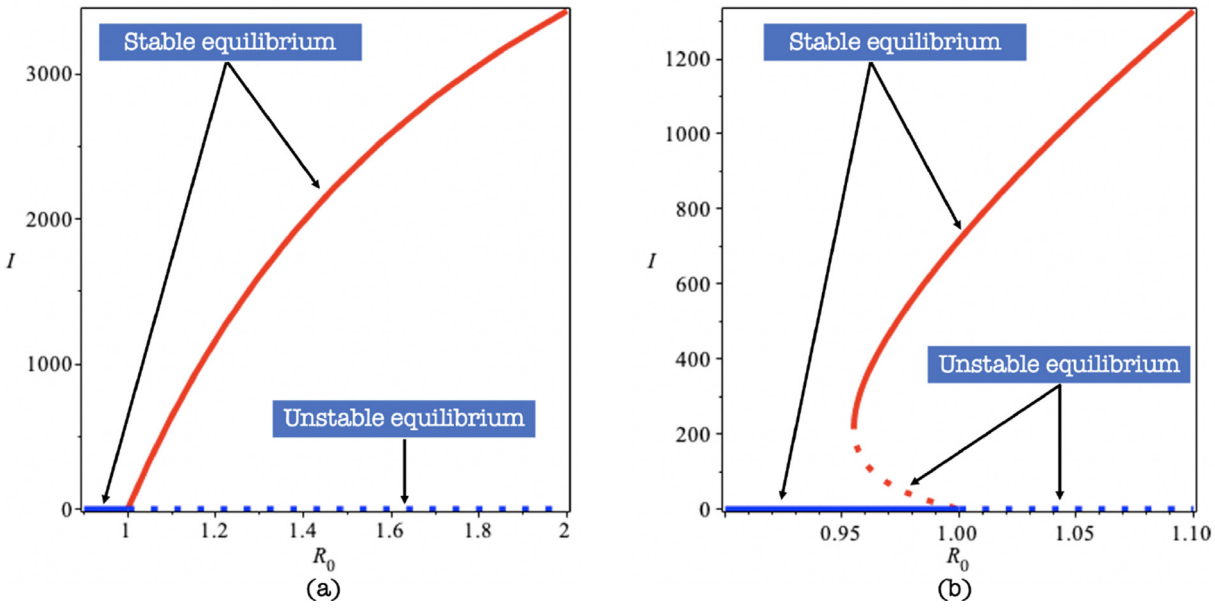

Fig. 4. Forward (a) and backward (b) bifurcation diagrams of system (1) showing the exchange of stability in $\mathscr{R}_0 = 1$. The red curve presents the COVID-19 endemic equilibrium point, while the blue curve indicates a COVID-19 free equilibrium point. (For interpretation of the references to colour in this figure legend, the reader is referred to the web version of this article.)

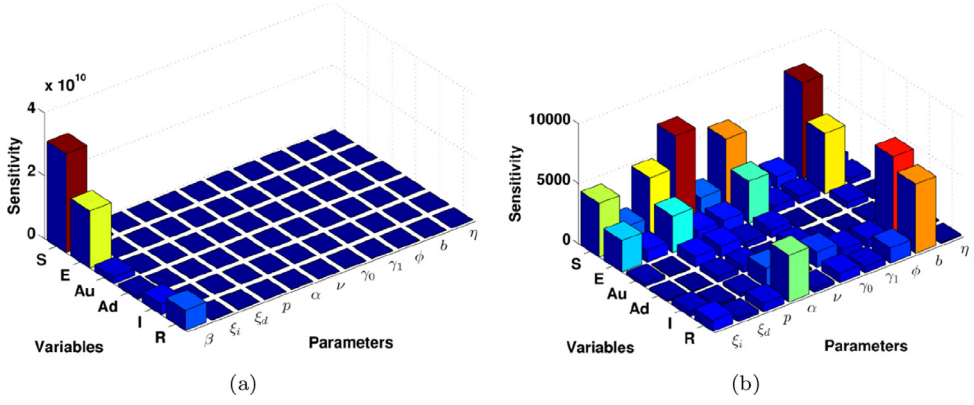

Fig. 5. Local sensitivity analysis with **non–normalization** technique in computational simulations using MATLAB for confirmed cases of the COVID-19 in Jakarta, (a) the sensitivity of all variables with respect to all parameters, (b) the sensitivity of all variables with respect to all parameters except β.

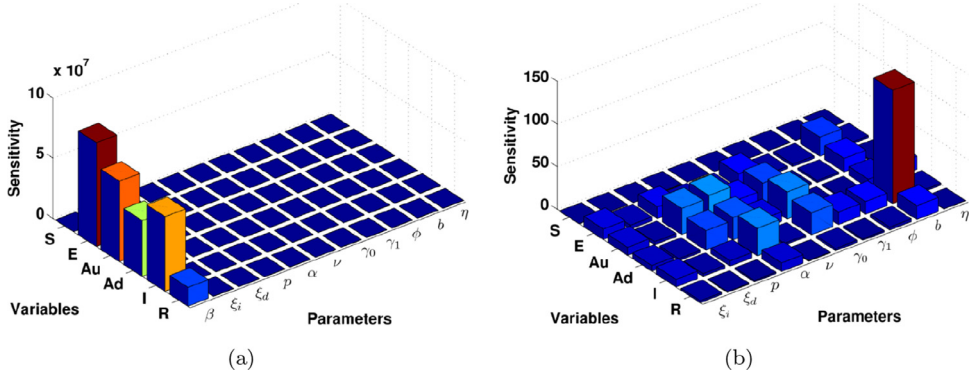

Fig. 6. Local sensitivity analysis with **half normalization** technique in computational simulations using MATLAB for confirmed cases of the COVID-19 in Jakarta, (a) the sensitivity of all variables with respect to all parameters, (b) the sensitivity of all variables with respect to all parameters except β.

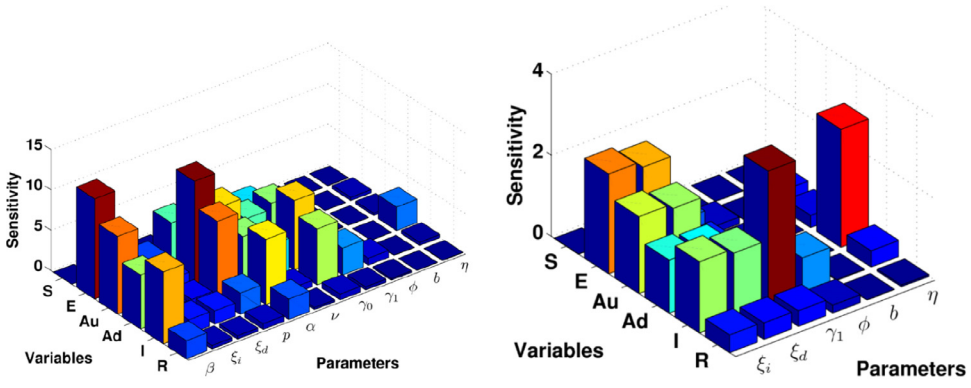

Fig. 7. Local sensitivity analysis with **full normalization** technique in computational simulations using MATLAB for confirmed cases of the COVID-19 in Jakarta, (a) the sensitivity of all variables with respect to all parameters, (b) the sensitivity of all variables with respect to parameters $\{\xi_i, \xi_d, \gamma_1, \phi, b, \eta\}$.

the most sensitive parameter in the suggested model is the infectious transmission rate β; see Figs. 5a. In addition, the susceptible and exposed individuals are also extremely sensitive to these parameters $\{\xi_i, p, \alpha, \gamma_0, b\}$, see Fig. 5b. By using a half normalization technique, the model states $\{E, A_u, A_d, I, R\}$ are extremely sensitive to the infectious transmission rate β, while they are less sensitive to the other parameters, see Fig. 6a and b. Furthermore, computational results show that the exposed infected, asymptomatic undetected individuals, asymptomatic detected individuals, symptomatic infected and recovered individuals are more sensitive to the set of parameters $\{\beta, p, \alpha, \nu, \gamma_0\}$ while they are less sensitive to the other model parameters, see Fig. 7a and b. This gives us how public health partners pay more attention priority on interventions for such groups.

Consequently, identification of the critical model parameters in this study based on computational simulations is an effective way to further study the model both practically and theoretically and to provide some suggestions for future improvements regarding COVID-19 transmissions, interventions, and control of the spread of the disease. It can be concluded that the person–to–person contact, the transmission rate, the progression rate of the incubation period, the effort for early detection through testing and the natural recovery rate may have a significant role in controlling this disease. Other factors also have a role to infect in the infection of people at different levels, as clearly indicated in our computational simulations.

6. Analyzing the plan for gradual relaxing of strict social distancing in the city of Jakarta, Indonesia

In Fig. 8, we present the estimation and actual incidence data of COVID-19 in Jakarta, from March 3, until May 10, and then the simulation continued for a longer period of time. Note that the policy of Jakarta government to conduct physical and social distancing was applied on April 10, 2020. Since April 10, the reduction of incidence occurs significantly. The physical distancing in Jakarta called PSBB (in Indonesian: *Pembatasan Sosial Berskala Besar* (large-scale social restriction)). It can be seen that, if social distancing intervention is maintained for a longer period of time, then the outbreak of COVID-19 in Jakarta will be significantly reduced, and delayed. With this intervention, the hospitals can treat infected individuals at a maximum capacity.

Recently, the Jakarta government has planned to relax the strict social distancing policy. This relaxed policy will be implemented in five-phases:

1. Phase 1: June 1- June 8. Industry and public services can operate based on the Covid-19 health protocol.
2. Phase 2: June 8, - June 15. Shopping centers may operate as before (shops may open), but under the COVID-19 health protocol.
3. Phase 3: June 15, - July 6. Similar to phase 2, but all the schools will not open simultaneously.
4. Phase 4: July 6, - July 20. Economic activities may be evaluated, for example, in case of restaurants and travel.
5. Phase 5: July 20, - July 27. Evaluation of the social activities on a large scale will be evaluated.

Based on this description, it is assumed that the transmission rate will increasing step by step from $\beta = 1.05 \times 10^{-7}$ (when social distancing implemented in April 10) to $\beta = 1.44 \times 10^{-7}$ (early infection period of data). To handle this, we assume β to be a step function as follows:

$$\beta(t) = 10^{-7} \times \begin{cases} 1.04 & \text{, Phase 1 : June 1,- June 8} \\ 1.14 & \text{, Phase 2 : June 8, - June 15} \\ 1.24 & \text{, Phase 3 : June 15, - July 6} \\ 1.34 & \text{, Phase 4 : July 6, - July 20} \\ 1.44 & \text{, Phase 5 : July 20, - July 27.} \end{cases} \tag{11}$$

Using above $\beta(t)$, the dynamics of $I(t)$ and $A_d(t)$ are shown in Fig. 9. It appears that the policy of relaxing the strict social distancing rule can result in an increasing number of new infections. However, it will not be as it was before social distancing was implemented. The possible explanation for this is that the policy for relaxing the social distancing is too early to take place.

Based on the elasticity analysis of $\mathscr{R}_0$ described in the previous section, rapid testing is one promising alternative for the eradication of COVID-19. Therefore, we simulated the results of the policy to relax the strict social distancing rules combined with a more rapid test intervention. To simulate this scenario, we use the same β as in (11), but increasing the rapid testing and hospitalization rate twice larger. The results are shown in Fig. 10. It can be seen that increasing rapid tests and hospitalization as a tolerance policy of relaxing the social distancing rules succeds in reducing the number of the infected population. Unfortunately, when the social distancing completely stops (after July 27), then the effect of rapid test and hospitalization is no longer able to compensate for the impact of relaxing the strict social distancing for the purpose of reducing the spread of COVID-19. Therefore, the number of the infected populations will start to re-increase and produce a new outbreak.

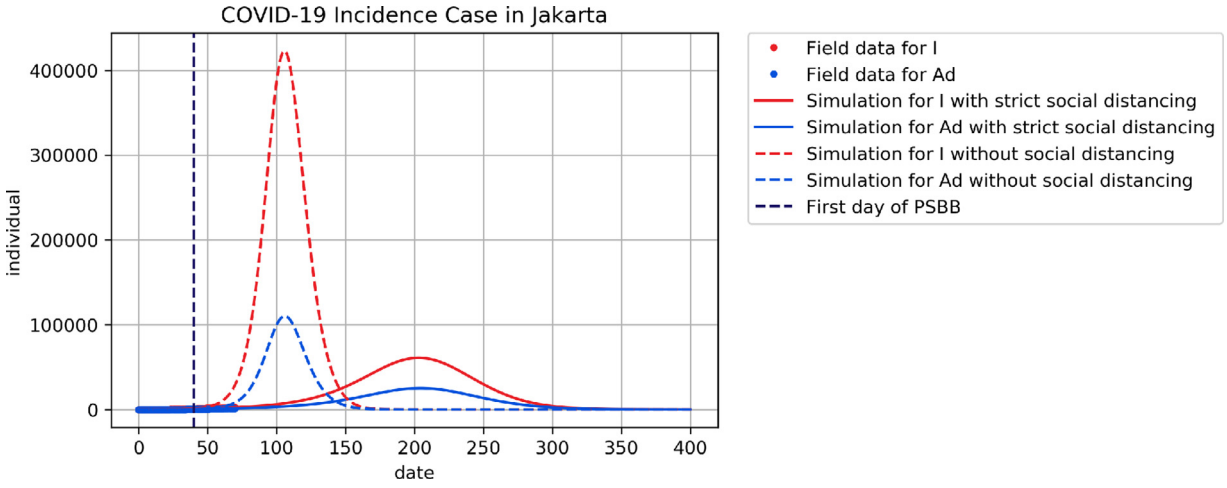

Fig. 8. A long-time simulation for the prediction of incidence of COVID-19 in Jakarta.

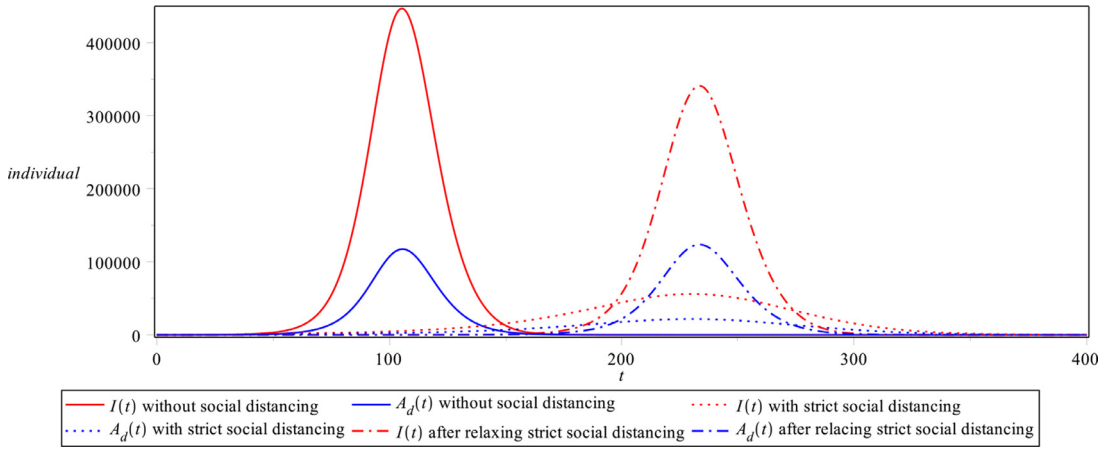

Fig. 9. Long-time simulation for prediction of incidence of COVID-19 in Jakarta with easing of social distancing policy.

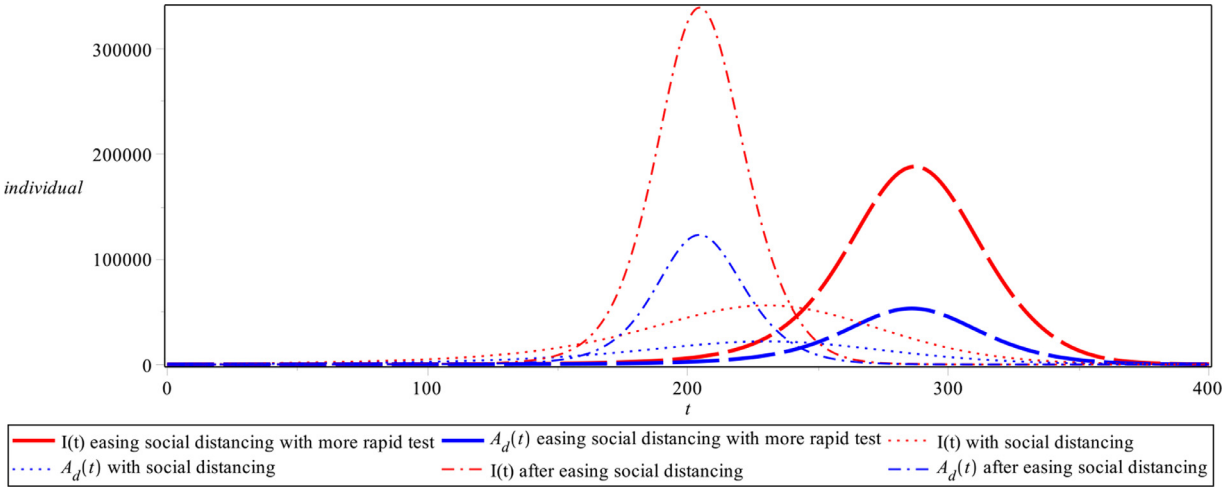

Fig. 10. Long-time simulation for prediction of incidence of COVID-19 in Jakarta with easing the social distancing policy combined with more massive rapid test and hospitalization.

7. Conclusions

A new deterministic compartmental model was constructed in this study to evaluate the spreading of COVID-19 among the human population. The model considers many important factors, such as hidden cases, rapid testing to trace hidden cases, limitation of medical resources, social distancing, quarantine/isolation, and parameter estimation for the incidence date from the city of Jakarta, Indonesia. The model consisted of six variables and was rigorously analyzed. A qualitative analysis of the model showed the following results.

1. The model exhibits two types of equilibrium points: COVID-19 free and COVID-19 endemic. The local stability of each equilibrium point depends on the basic reproduction number ($\mathscr{R}_0$). We found that the COVID-19-free equilibrium point is always locally asymptotically stable if $\mathscr{R}_0$ is less than unity.
2. A COVID-19-endemic equilibrium point always exists when $\mathscr{R}_0$ is larger than unity.
3. The model undergoes a backward bifurcation phenomenon at the associated $\mathscr{R}_0$ is equal to one , whenever the saturation parameter for hospitalization (b) is larger than a specific threshold (b^*). This means that whenever the medical resources are insufficient (larger b), the risk of the appearance of a backward bifurcation increases; this is related to the existence of the COVID-19-endemic equilibrium despite $\mathscr{R}_0 < 1$. Therefore, the success of the intervention also depends on the initial condition when the interventions is implemented. The study shows that increasing the capacity of a hospital or providing a considerably better quality of treatment in the hospital increases the probability of avoiding a backward bifurcation.

Numerical experiments of the model based on the incidence data of the city of Jakarta suggest the following.

1. The basic reproduction number in Jakarta during the early spread of COVID-19 is 1.75, which is larger than unity. This means that COVID-19 will persist in the population if no intervention is implemented by the government or the community.
2. From an analysis of the elasticity of $\mathscr{R}_0$, we observe that the infection rate (β) is the most significant controllable parameter to reduce $\mathscr{R}_0$, followed by the effectiveness of self-isolation and quarantine. Smaller values of these mentioned parameters will reduce $\mathscr{R}_0$, thereby increasing the chance of eradicating COVID-19 from the community.
3. The government must be careful when relaxing the policy of strict social distancing, particularly in terms of when it should be initiated. Mistakes in the prediction of when to start relaxing the social distancing policy can affect the emergence of a second outbreak.
4. A rapid test-based intervention has been proven to have potential in reducing $\mathscr{R}_0$ as an alternative approach, instead of relying solely on a lockdown or strict social distancing. Significantly better results might be obtained if these interventions can be implemented simultaneously.

During this pandemic, it is important to avoid overconfidence in the capabilities of the model for the long term prediction of the data. Many assumptions were made in the study to simplify the model without compromising the main objective. Although many important qualitative features were found from the model applied in this study, several limitations can still be found, and an alternative way to improve the model should be developed. One of the limitations in this study is that the applied model does not include the spatial spread of COVID-19 and the possibility of a relapse for recovered individuals. Further research is required in this field to address this limitation and a better modeling is needed to understand and anticipate the outcome of the COVID-19 pandemic.

Funding

1st author is funded by Universitas Indonesia with PUTI KI Q2 research grant scheme, ID No : NKB-775/UN2.RST/HKP.05.00/2020.

Declaration of Competing Interest

The authors declare that they have no known competing financial interests or personal relationships that could have appeared to influence the work reported in this paper.

Appendix A. Derivation of $\mathscr{R}_0$

The basic reproduction number $\mathscr{R}_0$ is calculated here by taking $E(t), A_u(t), A_d(t), I(t)$ as the infected compartments and then using the notation in [20] We define $\mathbf{T}$ as the transmission matrix and Σ as the transition matrix. The transmission and transition matrices of the corresponding linearized subsystem are four-dimensional, with

$$\mathbf{T} = \begin{pmatrix} 0 & \frac{\beta\,\Lambda}{\mu} & \frac{\beta\,\Lambda\,\xi_a}{\mu} & \frac{\beta\,\Lambda\,\xi_i}{\mu} \\ 0 & 0 & 0 & 0 \\ 0 & 0 & 0 & 0 \\ 0 & 0 & 0 & 0 \end{pmatrix}, \text{ and}$$

$$\Sigma = \begin{pmatrix} -\alpha-\mu & 0 & 0 & 0 \\ \alpha\,p & -\mu-\nu-\gamma_0 & 0 & 0 \\ 0 & \nu & -\eta-\mu-\gamma_0 & 0 \\ (1-p)\alpha & 0 & \eta & -\gamma_0-\gamma_1-\mu-\phi \end{pmatrix}.$$

It can be seen that T has three zero rows in row 2, 3 and 4. Therefore, the auxiliary matrix $\mathbf{E}$ is given by $\mathbf{E} = [1, 0, 0, 0]^T$. Hence, we have the next-generation matrix is given by

$$\begin{aligned} K &= -\mathbf{E}^T\mathbf{T}\Sigma^{-1}\mathbf{E}, \\ &= \left[\frac{\beta\,\Lambda\,\alpha\,[\xi_i(\eta\,\nu + (1-p)(\mu+\gamma_0)(\mu+\eta+\nu+\gamma_0)) + p(\mu+\phi+\gamma_0+\gamma_1)(\nu\,\xi_a+\eta+\mu+\gamma_0)]}{\mu\,(\mu+\phi+\gamma_0+\gamma_1)(\mu+\nu+\gamma_0)(\mu+\eta+\gamma_0)(\alpha+\mu)}\right]. \end{aligned}$$

The basic reproduction number as the spectral radius of K is given by

$$\mathcal{R}_0 = \frac{\beta\Lambda\alpha[\xi_i(\eta\nu + (1-p)(\mu+\gamma_0)(\mu+\eta+\nu+\gamma_0)) + p(\mu+\phi+\gamma_0+\gamma_1)(\nu\xi_a+\eta+\mu+\gamma_0)]}{\mu(\mu+\phi+\gamma_0+\gamma_1)(\mu+\nu+\gamma_0)(\mu+\eta+\gamma_0)(\alpha+\mu)}$$

Appendix B. Form of the COVID-19 endemic equilibrium

The COVID-19 endemic equilibrium point is given by

$$\begin{aligned} S^* &= \frac{(\mu+\nu+\gamma_0)(\eta+\mu+\gamma_0)(\alpha+\mu)(I^*\,b\mu + I^*\,b\phi + I^*\,b\gamma_0 + \mu+\phi+\gamma_0+\gamma_1)}{(1-p)\left(b\xi_i\left(\eta\,\nu+\eta\,\gamma_0+\mu^2+\mu\,\nu+2\,\mu\,\gamma_0+\nu\,\gamma_0+\gamma_0^2\right)I^* + (\gamma_0+\mu)(\gamma_0+\mu+\nu+\eta)\xi_i\right)+k_s}, \\ E^* &= \frac{I^*\,(\mu+\eta+\gamma_0)(I^*\,b\mu + I^*\,b\phi + I^*\,b\gamma_0 + \mu+\phi+\gamma_0+\gamma_1)(\mu+\nu+\gamma_0)}{\left(\left(\eta\,\mu+\eta\,\gamma_0+\mu^2+\mu\,\nu+2\,\mu\,\gamma_0+\nu\,\gamma_0+p\gamma_0^2\right)(1-p)+\eta\,\nu\right)(I^*\,b+1)\alpha}, \\ A_u^* &= \frac{(I^*\,b\mu + I^*\,b\phi + I^*\,b\gamma_0 + \mu+\phi+\gamma_0+\gamma_1)pI^*\,\nu}{\left(\left(\eta\,\mu+\eta\,\gamma_0+\mu^2+\mu\,\nu+2\,\mu\,\gamma_0+\nu\,\gamma_0+p\gamma_0^2\right)(1-p)+\eta\,\nu\right)(I^*\,b+1)}, \\ A_d^* &= \frac{I^*\,p(\mu+\eta+\gamma_0)(I^*\,b\mu + I^*\,b\phi + I^*\,b\gamma_0 + \mu+\phi+\gamma_0+\gamma_1)}{\left(\left(\eta\,\mu+\eta\,\gamma_0+\mu^2+\mu\,\nu+2\,\mu\,\gamma_0+\nu\,\gamma_0+p\gamma_0^2\right)(1-p)+\eta\,\nu\right)(I^*\,b+1)}, \\ R^* &= \frac{(\gamma_0+\mu+\nu+\eta)(I^*\,bp\phi\,\gamma_0 + (1-p)\mu\,\gamma_1 + p\phi\,\gamma_0) + b\gamma_0(\mu+\nu+\gamma_0)(\eta+\mu+\gamma_0)I^* + k_r}{(\delta+\mu)(I^*\,b+1)((1-p)(\gamma_0+\mu)(\gamma_0+\mu+\nu+\eta)+\eta\,\nu)}. \end{aligned}$$

and

$$\begin{aligned} k_s &= p(\xi_a\nu+\eta+\mu+\gamma_0)(I^*\,b\mu + I^*\,b\phi + I^*\,b\gamma_0 + \mu+\phi+\gamma_0+\gamma_1) \\ &+ I^*\,b\eta\,\mu\,\xi_i + \eta\,\mu\,\xi_i, \\ k_r &= \eta\,\mu\,\gamma_0 + \eta\,\nu\,\gamma_1 + \eta\,\gamma_0^2 + \eta\,\gamma_0\gamma_1 + \mu^2\gamma_0 + \mu\,\nu\,\gamma_0 \\ &+ 2\,\mu\,\gamma_0^2 + \nu\,\gamma_0^2 + \nu\,\gamma_0\gamma_1 + \gamma_0^3 + \gamma_0^2\gamma_1 + \nu\,\gamma_0. \end{aligned}$$

where I^* is taken from the positive roots of $\mathscr{P}(I)$.

Appendix C. Proof of Theorem 3

To show the possible existence of the COVID-19 endemic equilibrium point when $\mathscr{R}_0 < 1$, we analyze the sign of $\frac{\partial I}{\partial \mathscr{R}_0}$ when $\mathscr{R}_0 = 1$ and $I = 0$. If the sign is negative, then we have at least one COVID-19 endemic equilibrium point when $\mathscr{R}_0 < 1$ but close to 1. As the first step, each coefficient of a_i in $\mathscr{P}(I)$ is rewritten as a function of $\mathscr{R}_0$. To acchieve this, let

$$\beta^* = \mathcal{R}_0\frac{\mu\,(\mu+\phi+\gamma_0+\gamma_1)(\mu+\nu+\gamma_0)(\mu+\eta+\gamma_0)(\alpha+\mu)}{\Lambda\,\alpha\,[\xi_i(\eta\,\nu + (1-p)(\mu+\gamma_0)(\mu+\eta+\nu+\gamma_0)) + p(\mu+\phi+\gamma_0+\gamma_1)(\nu\,\xi_a+\eta+\mu+\gamma_0)]}.$$

Substitute β^* into a_i, then taking the implicit derivative of I with respect to $\mathscr{R}_0$ from $\mathscr{P}(I)$, we get :

$$\begin{aligned} &I^3\,\frac{\partial a_3(\mathcal{R}_0)}{\partial\mathcal{R}_0} + a_3(\mathcal{R}_0)\frac{\partial I^3}{\partial\mathcal{R}_0} + I^2\,\frac{\partial a_2(\mathcal{R}_0)}{\partial\mathcal{R}_0} + a_2(\mathcal{R}_0)\frac{\partial\,I^2}{\partial\mathcal{R}_0} \\ &+I\,\frac{\partial a_1(\mathcal{R}_0)}{\partial\mathcal{R}_0} + a_1(\mathcal{R}_0)\frac{\partial I}{\partial\mathcal{R}_0} + \frac{\partial a_0(\mathcal{R}_0)}{\partial\mathcal{R}_0} = 0. \end{aligned}$$

Substituting $I = 0, \mathscr{R}_0 = 1$, we have

$$\frac{\partial I}{\partial \mathscr{R}_0} = -\left(\frac{\partial a_0(\mathscr{R}_0)}{\partial \mathscr{R}_0}\right)\frac{1}{a_1(\mathscr{R}_0)}.$$

Since $\frac{\partial a_0(\mathscr{R}_0)}{\partial \mathscr{R}_0}$ is always negative, we have $\frac{\partial I}{\partial \mathscr{R}_0} < 0 \iff a_1(\mathscr{R}_0) < 0$, or equivalently $b < b^*$ where

$$b^* = \frac{\beta((1-p)\xi_i(\mu+\gamma_0)(\eta+\mu+\nu+\gamma_0) - p(\mu+\phi+\gamma_0+\gamma_1)(\nu\,\xi_a+\eta+\mu+\gamma_0) - \eta\,\nu\,\xi_i)k_{b_1}}{(\mu+\delta)((1-p)(\mu+\gamma_0)(\eta+\mu+\nu+\gamma_0) - \eta\,\nu)k_{b_2}},$$

and $\beta = \beta^*$, with

$$\begin{aligned}
k_{b_1} &= (\eta+\mu+\nu+\gamma_0)((1-p)\alpha\,\delta\,\phi\,\gamma_0 + \alpha\,\delta\,\mu\,\gamma_1 p)\\
&+ (\mu+\phi+\gamma_0+\gamma_1)(\mu+\nu+\gamma_0)\left(\eta\,\mu^2 + \mu^2(\mu+\gamma_0) + \alpha\,\eta\,\mu\right)\\
&+ \gamma_0(\phi+\gamma_0+\gamma_1)(\nu+\gamma_0) + \alpha\,\mu\,\phi\,\gamma_0^2\\
&+ \alpha\,\delta\left(\left(\mu^2+\mu\,\nu+\mu\,\phi+\mu\,\gamma_0+\nu\,\phi\right)\eta + \mu\,(\mu+\phi+\gamma_0)(\mu+\nu+\gamma_0)\right)\\
&+ \left((\mu+\nu+\phi+2\,\gamma_0+\gamma_1)\eta + \mu^2\right)\mu + \eta\,(\phi+\gamma_0+\gamma_1)(\nu+\gamma_0)\\
&+ \alpha^2\mu^5\gamma_0^2\gamma_1 + \alpha\,\mu^3(\nu+\phi+3\gamma_0+\gamma_1) + \alpha\,\mu^2\nu(\phi+2\,\gamma_0+\gamma_1)\\
&+ \alpha\,\mu\,\gamma_0^3 + \alpha\,\mu^2\left(2\phi\,\gamma_0 + 3\gamma_0^2 + 2\gamma_0\gamma_1\right) + \alpha\,\mu\,\nu\,\gamma_0(\phi+\gamma_0+\gamma_1)\\
k_{b_2} &= 2\,(1-p)\Lambda\,\alpha\,\xi_i(\mu+\gamma_0)(\eta+\mu+\nu+\gamma_0)\\
&+ -\Lambda\,\alpha\,(2\,\mu+2\,\phi+2\,\gamma_0+\gamma_1)(\nu\,\xi_a+\eta+\mu+\gamma_0)p\\
&+ \mu\,(2\,\mu+2\,\phi+2\,\gamma_0+\gamma_1)(\mu+\nu+\gamma_0)(\mu+\eta+\gamma_0)(\mu+\alpha).
\end{aligned}$$

Appendix D. Proof of Theorem 4

The backward bifurcation is shown using the concept of the center manifold theory on system (1). To use the center manifold theory, we make the following changes to the variables. Let $S = x_1$, $E = x_2$, $A_u = x_3$, $A_d = x_4$, $I = x_5$ and $R = x_6$ and let β the bifurcation parameter. Denote $x = (x_1, x_2, x_3, x_4, x_5, x_6)^T$ and $\frac{dx}{dt} = (f_1, f_2, f_3, f_4, f_5, f_6)^T$ as given below

$$\begin{aligned}
\frac{dx_1}{dt} &= \Lambda - \beta S(A_u + \xi_i I + \xi_a A_d) - \mu S + \delta R := f_1,\\
\frac{dx_2}{dt} &= \beta S(A_u + \xi_i I + \xi_a A_d) - \alpha E - \mu E := f_2,\\
\frac{dx_3}{dt} &= p\alpha E - uA_u - \gamma_0 A_u - \mu A_u := f_3,\\
\frac{dx_4}{dt} &= uA_u - \gamma_0 A_d - \eta A_d - \mu A_d := f_4,\\
\frac{dx_5}{dt} &= (1-p)\alpha E + \eta A_d - \left(\gamma_0 + \frac{\gamma_1}{1+bI}\right)I - \mu I - \phi I := f_5,\\
\frac{dx_6}{dt} &= \gamma_0(A_u + A_d) + \left(\gamma_0 + \frac{\gamma_1}{1+bI}\right)I - \mu R - \delta R := f_6,
\end{aligned} \tag{D.1}$$

The Jacobian of system (D.1) evaluated at the disease-free equilibrium, $D_x f$ is given by

$$\begin{pmatrix}
-\mu & 0 & -\frac{\beta\,\Lambda}{\mu} & -\frac{\beta\,\Lambda\,\xi_a}{\mu} & -\frac{\beta\,\Lambda\,\xi_i}{\mu} & \delta\\
0 & -\alpha-\mu & \frac{\beta\,\Lambda}{\mu} & \frac{\beta\,\Lambda\,\xi_a}{\mu} & \frac{\beta\,\Lambda\,\xi_i}{\mu} & 0\\
0 & \alpha\,p & -\mu-\nu-\gamma_0 & 0 & 0 & 0\\
0 & 0 & \nu & -\eta-\mu-\gamma_0 & 0 & 0\\
0 & (1-p)\alpha & 0 & \eta & -\gamma_0-\gamma_1-\mu-\phi & 0\\
0 & 0 & \gamma_0 & \gamma_0 & \gamma_0+\gamma_1 & -\mu-\delta
\end{pmatrix}$$

Consider the case $\mathscr{R}_0 = 1$. Suppose that β is chosen as a bifurcation parameter. Setting $\mathscr{R}_0 = 1$ and solving for β gives

$$\beta^* = \frac{\mu\,(\alpha+\mu)(\mu+\nu+\gamma_0)(\eta+\mu+\gamma_0)(\gamma_0+\gamma_1+\mu+\phi)}{\Lambda\,\alpha\,(\xi_i(\nu\,\eta+(1-p)(\mu+\gamma_0)(\mu+\eta+\nu+\gamma_0)) + p(\gamma_0+\gamma_1+\mu+\phi)(\nu\,\xi_a+\eta+\mu+\gamma_0))}.$$

The Jacobian matrix $D_x f$ evaluated at $\beta = \beta^*$ has a simple zero eigenvalue, and the other eigenvalues have negative real parts.

The right and the left eigenvector which associated with a zero eigenvalue are denoted respectively by $\vec{\omega} = (\omega_1, \omega_2, \omega_3, \omega_4, \omega_5, \omega_6)^T$ and $\vec{v} = (v_1, v_2, v_3, v_4, v_5, v_6)^T$, we have

$$\begin{aligned}
\omega_1 &= \frac{\omega_5\alpha\,\delta\,(\mu+\eta+\nu+\gamma_0)(\mu\,p\gamma_1+(1-p)\phi\,\gamma_0)+C}{((p-1)(\mu+\gamma_0)(\mu+\eta+\nu+\gamma_0)-\nu\,\eta)(\delta+\mu)\alpha\,\mu},\\
\omega_2 &= \frac{(\gamma_0+\gamma_1+\mu+\phi)(\mu+\nu+\gamma_0)(\eta+\mu+\gamma_0)\omega_5}{\alpha\,(\nu\,\eta+(1-p)(\mu+\gamma_0)(\mu+\eta+\nu+\gamma_0))},\\
\omega_3 &= \frac{(\eta+\mu+\gamma_0)\omega_5 p(\gamma_0+\gamma_1+\mu+\phi)}{\nu\,\eta+(1-p)(\mu+\gamma_0)(\mu+\eta+\nu+\gamma_0)},\\
\omega_4 &= \frac{\omega_5\nu\,p(\gamma_0+\gamma_1+\mu+\phi)}{\nu\,\eta+(1-p)(\mu+\gamma_0)(\mu+\eta+\nu+\gamma_0)},\\
\omega_5 &= \omega_5,\\
\omega_6 &= \frac{\left((\eta+\mu+\nu+\gamma_0)((1-p)\mu\,\gamma_1-\phi\,\gamma_0)-\gamma_0^3-(2\,\mu+\nu+\eta+\gamma_1)\gamma_0^2\right)}{\nu\,\eta+(1-p)(\mu+\gamma_0)(\eta+\mu+\nu+\gamma_0)(\delta+\mu)}\\
&- \frac{\omega_5((\mu+\eta)(\mu+\nu)\gamma_0-\eta\,\nu\,\gamma_1-((+\mu+\nu+\eta)\gamma_1)\gamma_0)}{\nu\,\eta+(1-p)(\mu+\gamma_0)(\eta+\mu+\nu+\gamma_0)(\delta+\mu)}
\end{aligned}$$

where C has a long expression with a positive sign, and

$$\begin{aligned}
v_1 = v_6 &= 0,\\
v_2 &= \frac{(1-p)p\xi_i(\mu+\gamma_0)(\mu+\eta+\nu+\gamma_0)+\eta\,\nu\,\xi_i+p(\gamma_0+\gamma_1+\mu+\phi)(\nu\,\xi_a+\eta+\mu+\gamma_0)}{\xi_i(\mu+\nu+\gamma_0)(\eta+\mu+\gamma_0)(\alpha+\mu)}\\
v_3 &= \frac{\left(\gamma_0^2+(\nu\,\xi_a+\eta+2\,\mu+\phi+\gamma_1)\gamma_0+\mu^2+(\nu\,\xi_a+\eta+\phi+\gamma_1)\mu+(\nu\,\xi_i+\phi+\gamma_1)\eta+\nu\,\xi_a(\gamma_1+\phi)\right)v_5}{(\eta+\mu+\gamma_0)(\mu+\nu+\gamma_0)\xi_i},\\
v_4 &= \frac{(\eta\,\xi_i+\mu\,\xi_a+\phi\,\xi_a+\gamma_0\xi_a+\gamma_1\xi_a)v_5}{(\eta+\mu+\gamma_0)\xi_i}\\
v_5 &= v_5
\end{aligned}$$

Next we will calculate the values of $\mathcal{A}$ and $\mathcal{B}$. Since $v_1 = v_6 = 0$, we only need to compute the partial derivatives of f_2,f_3,f_4,f_5 at the COVID-19 free equilibrium. For system (D.1) the associated non-zero partial derivatives of f_2,f_3,f_4,f_5 are given by

$$\frac{\partial^2 f_2}{\partial x_1\partial x_3} = \frac{\partial^2 f_2}{\partial x_3\partial x_1} = \beta, \qquad \frac{\partial^2 f_2}{\partial x_1\partial x_4} = \frac{\partial^2 f_2}{\partial x_4\partial x_1} = \beta\,\xi_a,$$

$$\frac{\partial^2 f_2}{\partial x_1\partial x_5} = \frac{\partial^2 f_2}{\partial x_5\partial x_1} = \beta\,\xi_i, \qquad \frac{\partial^2 f_5}{\partial x_5\partial x_5} = 2\,\gamma_1\,b.$$

It follows that

$$\begin{aligned}
\mathcal{A} &= v_2\sum_{i,j=1}^{6}\omega_i\omega_j\frac{\partial^2 f_2}{\partial x_i\partial x_j}+v_3\sum_{i,j=1}^{6}\omega_i\omega_j\frac{\partial^2 f_3}{\partial x_i\partial x_j}+v_4\sum_{i,j=1}^{6}\omega_i\omega_j\frac{\partial^2 f_4}{\partial x_i\partial x_j}+v_5\sum_{i,j=1}^{6}\omega_i\omega_j\frac{\partial^2 f_5}{\partial x_i\partial x_j},\\
&= v_2\,\omega_1\left(2\,\frac{\nu\,p(\gamma_0+\gamma_1+\mu+\phi)\beta\,\xi_a}{\nu\,\eta+(1-p)(\mu+\gamma_0)(\mu+\eta+\nu+\gamma_0)}+2\,\frac{(\eta+\mu+\gamma_0)p(\gamma_0+\gamma_1+\mu+\phi)\beta}{\nu\,\eta+(1-p)(\mu+\gamma_0)(\mu+\eta+\nu+\gamma_0)}\right)\\
&+ v_2\,\omega_1\,2\,\beta\,\xi_i+2\,\gamma_1 b.
\end{aligned}$$

For the sign of $\mathcal{B}$, the association non-vanishing partial derivatives of f_2,f_3,f_4,f_5 are

$$\frac{\partial^2 f_2}{\partial x_3\partial\beta^*} = \frac{\Lambda}{\mu}, \frac{\partial^2 f_2}{\partial x_4\partial\beta^*} = \frac{\Lambda\,\xi_a}{\mu}, \frac{\partial^2 f_2}{\partial x_5\partial\beta^*} = \frac{\Lambda\,\xi_i}{\mu}.$$

It also follows that

$$\begin{aligned}
\mathcal{B} &= v_2\sum_{i=1}^{6}\omega_i\frac{\partial^2 f_2}{\partial x_i\partial\beta^*}+v_3\sum_{i=1}^{6}\omega_i\frac{\partial^2 f_3}{\partial x_i\partial\beta^*}+v_4\sum_{i=1}^{6}\omega_i\frac{\partial^2 f_4}{\partial x_i\partial\beta^*}+v_5\sum_{i=1}^{6}\omega_i\frac{\partial^2 f_5}{\partial x_i\partial\beta^*},\\
&= v_2\left(\frac{(\gamma_0+\gamma_1+\mu+\phi)(\mu+\nu+\gamma_0)(\eta+\mu+\gamma_0)\Lambda}{\alpha\,(\nu\,\eta+(1-p)(\mu+\gamma_0)(\mu+\eta+\nu+\gamma_0))\mu}+\frac{\nu\,p(\gamma_0+\gamma_1+\mu+\phi)\Lambda\,\xi_a}{(\nu\,\eta+(1-p)(\mu+\gamma_0)(\mu+\eta+\nu+\gamma_0))\mu}\right)\\
&+ \frac{v_2\,\Lambda\,\xi_i}{\mu}.
\end{aligned}$$

The coefficient $\mathcal{B}$ is clearly positive; the presence of backward bifurcation in the model (1) is determined by the sign of coefficient $\mathcal{A}$. Therefore, to conduct a backward bifurcation $\mathcal{A}$ should be positive, which gives us $b > b^*$ where b^* is given in Theorem 3.

CRediT authorship contribution statement

Dipo Aldila: Conceptualization, Methodology, Formal analysis, Software, Investigation, Validation, Writing - original draft, Writing - review & editing. **Sarbaz H.A. Khoshnaw:** Software, Conceptualization, Writing - original draft. **Egi Safitri:** Formal analysis, Investigation, Writing - original draft. **Yusril Rais Anwar:** Software, Investigation. **Aanisah R.Q. Bakry:** Software, Data curation. **Brenda M. Samiadji:** Investigation, Validation, Writing - original draft. **Demas A. Anugerah:** Software, Conceptualization, Writing - original draft. **M. Farhan Alfarizi GH:** Data curation, Validation. **Indri D. Ayulani:** Writing - original draft, Data curation. **Sheryl N. Salim:** Investigation, Data curation.

References

[1] Susilo A, Rumende CM, Pitoyo CW, Santoso WD, Yulianti M, Herikurniawan H, et al. Coronavirus disease 2019: tinjauan literatur terkini. Jurnal Penyakit Dalam Indonesia 2020;7(1):45–67.
[2] WHO. Pertanyaan dan jawaban terkait coronavirus, https://www.who.int/indonesia/news/novel-coronavirus/qa-for-public.
[3] WHO. Report of the who-china joint mission on coronavirus disease 2019 (COVID-19).. Tech. Rep.. World Health Organization; 2020.
[4] Covid-19 strategy update Tech. Rep.. World Health Organization; 2020.
[5] Lee D, Lee J. Testing on the move South Korea's rapid response to the COVID-19 pandemic. Trans Res InterdiscipPerspect 2020:100–11.
[6] M. of Health, W.R. of Korea. Coronavirus disease-19, Republic of Korea. http://ncov.mohw.go.kr/en/.
[7] Thakur V, Jain A. COVID 2019-suicides: a global psychological pandemic. Brain Behav Immun 2020.
[8] Ndairou F, Area I, Nieto JJ, Torres DF. Mathematical modeling of COVID-19 transmission dynamics with a case study of Wuhan. Chaos Solitons Fractals 2020;135:109846.
[9] Ivorra B, Ferrández MR, Vela-Pérez M, Ramos A. Mathematical modeling of the spread of the coronavirus disease 2019 (COVID-19) taking into account the undetected infections. the case of China. Commun Nonlinear Sci Numer Simul 2020:105303.
[10] Liu Z, Magal P, Seydi O, Webb G. A COVID-19 epidemic model with latency period. Infect Dis Modell 2020;5:323–37.
[11] Zu J, Li M, Li Z, Shen M, Xiao Y, Ji F. Epidemic trend and transmission risk of SARS-CoV-2 after government intervention in the mainland of China: a mathematical model study. Available at SSRN 35396692020.
[12] Tang B, Wang X, Li Q, Bragazzi NL, Tang S, Xiao Y, et al. Estimation of the transmission risk of the 2019-nCoV and its implication for public health interventions. J Clin Med 2020;9(2):462.
[13] Tang B, Bragazzi NL, Li Q, Tang S, Xiao Y, Wu J. An updated estimation of the risk of transmission of the novel coronavirus (2019-nCoV). Infect Dis Modell 2020;5:248–55.
[14] Mandal M, Jana S, Nandi SK, Khatua A, Adak S, Kar T. A model based study on the dynamics of COVID-19: prediction and control. Chaos Solitons Fractals 2020;6.
[15] Chatterjee K, Chatterjee K, Kumar A, Shankar S. Healthcare impact of COVID-19 epidemic in india: astochastic mathematical model. Med J Armed Forces India 2020;76(2):147–55.
[16] Zhao Z, Li X, Liu F, Zhu G, Ma C, Wang L. Prediction of the COVID-19 spread in African countries and implications for prevention and controls: a case study in South Africa, Egypt, Algeria, Nigeria, Senegal and Kenya. Sci Total Environ 2020:138959.
[17] Ceylan Z. Estimation of COVID-19 prevalence in Italy, Spain, and France. Sci Total Environ 2020;729:138817.
[18] Chintalapudi N, Battineni G, Amenta F. COVID-19 disease outbreak forecasting of registered and recovered cases after sixty day lockdown in Italy: a data driven model approach. J Microbiol Immunol Infect 2020.
[19] Chakraborty T, Ghosh I. Real-time forecasts and risk assessment of novel coronavirus (COVID-19) cases: a data-driven analysis. Chaos Solitons Fractals 2020;135.
[20] Diekmann O, Heesterbeek JAP, Roberts M. The construction of next-generation matrices for compartmental epidemic models. J R Soc Interface 2010:873–85.
[21] Driessche PV, Watmough J. Reproduction numbers and sub-threshold endemic equilibria for compartmental models of disease transmission. Math Biosci 2002:29–48.